Journal of Alloys and Compounds 509 (2011) L59–L62

Contents lists available at ScienceDirect

Journal of Alloys and Compounds

journal homepage: www.elsevier.com/locate/jallcom

Letter

Solvent effects in the synthesis of $MgFe_2O_4$ nanopowders by reverse micelle processing

J. Chandradass, Ki Hyeon Kim*

Department of Physics, Yeungnam University, Gyeongsan, Gyeongsangbuk-do 712-749, South Korea

ARTICLE INFO

Article history:
Received 8 July 2010
Received in revised form 15 October 2010
Accepted 21 October 2010
Available online 30 October 2010

Keywords:
Ferrites
Reverse micelle
Particle size
Magnetic property

ABSTRACT

Nanopowders of $MgFe_2O_4$ have been synthesized by the novel and facile reverse microemulsion route. The effects of changing the continuous phase on the particle size and the magnetic property have been studied. The average particle size, morphology and saturation magnetization are shown to be dependent on the continuous phase. The average diameters of the particle prepared with heptane are 20.9 ± 4.3 nm. On the contrary, the product with toluene and cyclohexane is highly aggregated. The values of saturation magnetization for our samples prepared with heptane, toluene and cyclohexane are 14.5, 30 and 37 emu/g.

1. Introduction

Magnetic fine particles have been a major research focus because of their many technological applications [1–6]. One interesting application of magnetic materials is in hyperthermia treatment which is considered as a supplementary treatment to chemotherapy, radiotherapy, and surgery in cancer therapy [7]. $MgFe_2O_4$ is one such material which has novel magnetic properties, particularly superparamagnetic behaviors [8], and such superparamagnetic particles can be used for different biomedical application. It was reported that $MgFe_2O_4$ particles whose size was several μm has relative high heat generation compared with other ferrites [9]. Therefore, it seems that $MgFe_2O_4$ nanoparticles with a precise size control have great capability for magnetic hyperthermia. The heating property in the AC magnetic field is strongly influenced by the particle size [10]. Synthesis using reverse micelles seems especially suited to tailoring particle properties at the nanolevel. In these systems nanodrops (3–30 nm) of the aqueous phase are trapped within aggregate of surface active molecules dispersed in an external oil phase [11–13]. Several group reported the synthesis of $NiFe_2O_4$ [14], $MnFe_2O_4$ [15,16], Ni and Zn ferrites [17] and mixed ferrites by reverse micelle process [17–22]. Recently, Sivakumar et al. [23] synthesized nanostructured $MgFe_2O_4$ spinel with various grain sizes ranging from 72 to 19 nm using ceramic method and followed by high-energy ball milling. Hankare et al. [24] synthesized $MgFe_2O_4$ by coprecipitation method with grain size of 40 nm. Sasaki et al. [25] produced magnesium ferrite ($MgFe_2O_4$) nanoparticles by hydrothermal synthesis in supercritical water with particle size of about 20 nm and saturation magnetization of 20 emu/g. Holec et al. [26] produced $MgFe_2O_4$ nanocrystals with intermediate phase (MgO) by reverse micelle method at 900 °C with particle size and saturation magnetization of 39 nm and 32 emu/g respectively. Although, the nanosized spinels of $MgFe_2O_4$ were prepared by reverse micelle method, some improvement or optimization of parameter is still required to control the particle size. The micellar exchange rate is varied by varying the continuous medium and by varying water to surfactant molar ratio (R) [27]. In this paper we have attempted to study the effects of changing the continuous medium on the particle size and the magnetic property of $MgFe_2O_4$ nanopowders.

2. Experimental

All chemicals in this work, such as (i) magnesium nitrate hexahydrate ($Mg(NO_3)_2{\cdot}6H_2O$, Sigma–Aldrich), (ii) iron (III) nitrate nonhydrate ($Fe(NO_3)_3{\cdot}9H_2O$, Aldrich), (iii) poly (oxyethylene) nonylphenyl ether (a nonionic surfactant, Igepal CO-520, Aldrich Chemical Co.), (iv) NH_4OH (33%) (Sigma–Aldrich), (v) heptane (Sigma–Aldrich), (vi) toluene (Sigma–Aldrich), (vii) cyclohexane (Sigma–Aldrich) were of analytical grade and used as received without further purification.

For the reverse micelle synthesis, a solution comprised of heptane, water, and a surfactant Poly(oxyethylene) nonylphenyl ether was used to form the micelles. For $MgFe_2O_4$ ferrite, an aqueous solution was prepared by mixing 80 ml of poly(oxyethylene) nonylphenyl ether, 200 ml of heptane and 39 ml of mixed aqueous salt solution. The molar ratio of water to surfactant ratio (R) was maintained at 12. Reverse microemulsion was prepared in a similar way for different solvents such as toluene and cyclohexane. The microemulsion was mixed rapidly, and after 5 min of equilibration, 18 ml of NH_4OH was injected into the microemulsion. The microemulsion was centrifuged to extract the particles, and the particles were sub-

* Corresponding author. Tel.: +82 53 810 2334; fax: +82 53 810 4616.
E-mail address: kee1@ynu.ac.kr (K.H. Kim).

0925-8388/$ – see front matter © 2010 Elsevier B.V. All rights reserved.
doi:10.1016/j.jallcom.2010.10.090

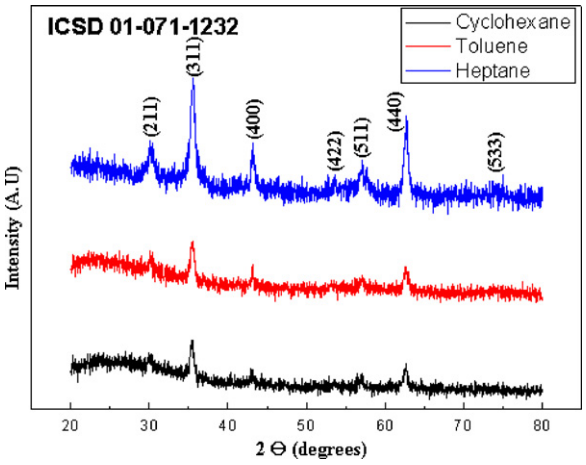

Fig. 1. X-ray diffraction patterns of $MgFe_2O_4$ samples calcined at 600 °C.

sequently washed by ethanol to remove any residual surfactant. The powders were dried at 80 °C in an oven for 24 h, grounded and calcined at 600 °C for 2 h.

The phase identification of calcined powders was recorded by X-ray diffractometer (Panalytical X'pert MPD). Field emission transmission electron microscopy measurements of the samples were taken on a JEOL-3010 instrument with a 300 kV accelerating voltage. The average diameter of the particle estimated from the TEM micrograph using standard software (IMAGE J). The magnetic measurement of the samples was performed on a superconducting quantum interference device magnetometer (Quantum design, MPMS XL-7).

3. Results and discussion

3.1. Structural analysis of $MgFe_2O_4$ nanoparticles by XRD, TEM

Fig. 1 shows the XRD pattern of $MgFe_2O_4$ nanoparticles synthesized with different solvent. The sharp peaks from diffraction pattern show the crystalline nature of the samples. The diffraction peaks could be ascribed to Bragg reflections of (1 1 1), (2 2 0), (3 1 1), (2 2 2), (4 0 0), (4 2 2), (5 1 1), and (4 4 0) planes which can be readily indexed to the spinel phase of bulk $MgFe_2O_4$ (ICSD-01-1232). The reflections are comparatively broader, revealing the nanosize of the crystals. According to the Debye–Scherrer equation, the average crystallite size was determined from the half-width of the most intense peak (3 1 1). The average crystalline sizes of 12.4 nm (heptane), 14.6 nm (toluene) and 15.4 nm (cyclohexane) were produced. The micellar dynamics is affected by changing the chain length of the oil phase. The longer the chain length of the oil, the more difficult it is to penetrate into the surfactant tail and align itself parallel to the surfactant tails. As a result, the extent of interaction between surfactant tail and the solvent chain decreases with an increase in chain length of the alkyl solvent. On the other hand, interdroplet tail–tail interaction of two surfactant molecules increases, due to the weak presence of solvent molecules in the tail region of the droplet. The net effect results in an increase in the micellar exchange rate with an increase in the chain length of the alkyl solvent [27]. Natrajan et al. [28] and Hatton et al. [29] studies haves shown that the final particle size is a function of the water to surfactant molar ratio (R), the concentration of the reactant species, the ion occupancy number, the initial distribution of the reactant, the water size core, and the intermicellar exchange coefficient. In our experiments we have kept the water to surfactant molar ratio and the concentration of reactant species the same in all cases. Therefore, the only parameter that can influence the particle size is the intermicellar exchange rate coefficient. In the case of cyclohexane, the molecules penetrate between surfactant tails, leading to an increase in surfactant curvature and rigidity and hence the exchange rate is low. The slow exchange rate adversely affects the formation of metal atoms. Therefore the nucleation and growth processes continue in parallel, resulting in a larger size of the particle [27]. In the case of toluene, the exchange rate coefficient increases by a three order of magnitude compared to cyclohexane. At high exchange rate, due to rapid collision between micelles there will be rapid exchange of material, which results in the formation of a large number of micelles with the number of magnesium ferrite atoms greater than the critical nucleation. This will result in smaller particle size, as the number of magnesium ferrite atoms left for growth will be relatively low. In the case of heptane the exchange rate coefficient decreases by a two order of magnitude from toluene. Slow exchange of materials will lead to formation of a smaller number of nuclei of magnesium ferrite. Consequently, a higher amount of magnesium ferrite atoms as compared to that in the case of toluene will be available for growth. Hence the terminal particle size is found to be larger than that in the case of toluene [27]. Fig. 2 shows the transmission electron microscopy (TEM) image of $MgFe_2O_4$ nanoparticles synthesized with heptane and the particle size distribution is included as inset. The digitized images were imported into the program, Image J and the populations of particles with respect to mean particle diameter were determined. 34 Particles were measured from TEM micrograph to establish particle size distribution histograms. The histograms were created using Image J with binning widths of 5 nm. The mean sizes and standard deviations resulted from Image J are 20.9 nm and 4.3 nm, respectively. On the contrary, the product with toluene and cyclohexane (Fig. 2(b) and (c)) is highly aggregated. The average particle size obtained from TEM is bigger than that observed from X-ray line broadening technique. This may be due to the agglomeration of fine particles [30].

3.2. Magnetic properties

Fig. 3 shows the room temperature magnetization curves of the $MgFe_2O_4$ nanoparticles prepared with different solvent. The M–H hysteresis loops indicating superparamagnetic property at a temperature of 300 K. The absence of hysteresis, negligible coercivity and remanance, and the nonattainment of saturation even at high magnetic field are the characteristics of superparamagnetic behavior. The superparamagnetic behavior at room temperature, meaning that the thermal energy can overcome the anisotropy energy barrier of a single particle and the net magnetization of the particles in the absence of an external field is zero [31]. The value of magnetization for our samples prepared with heptane, toluene and cyclohexane are 14.5, 30 and 37 emu/g. The relatively higher saturation value for $MgFe_2O_4$ ferrite nanocrystals prepared with cyclohexane may be due to the fact that the anisotropic features of these nanocrystals have enhanced dipole–dipole interaction, favoring a head-to-tail orientation, thus resulting in a relatively higher saturation value [32]. On the other hand, the magnetic saturation value for the nanocrystals prepared with heptane was found to be 14.5 emu/g, respectively. It is well-known that the magnetic properties of nanocrystals are predominantly dictated by the intrinsic properties of materials such as the anisotropy and saturation magnetization. Surface effects can lead to a decrease of the magnetization of small particles with respect to the bulk value. This reduction has been associated with different mechanisms, such as the existence of a magnetically dead layer on the particle's surface or the existence of spin glass like behavior of the surface spins [33]. The existence of some degree of spin canting in the whole volume of the particle, in addition to the disordered surface layer, could be an alternative explanation of this additional decrease of the saturation magnetization [18]. Liu et al. [34] reported the synthesis of $MgFe_2O_4$ nanoparticles at 600 °C from water in toluene reverse micelle using sodium dodecylbenzenesulfonate (NaDBS) and Cetyltrimethylammonium bromide (CTAB) as surfactants with a saturation magnetization of ~2.5 emu/g. Recently, Holec et al.

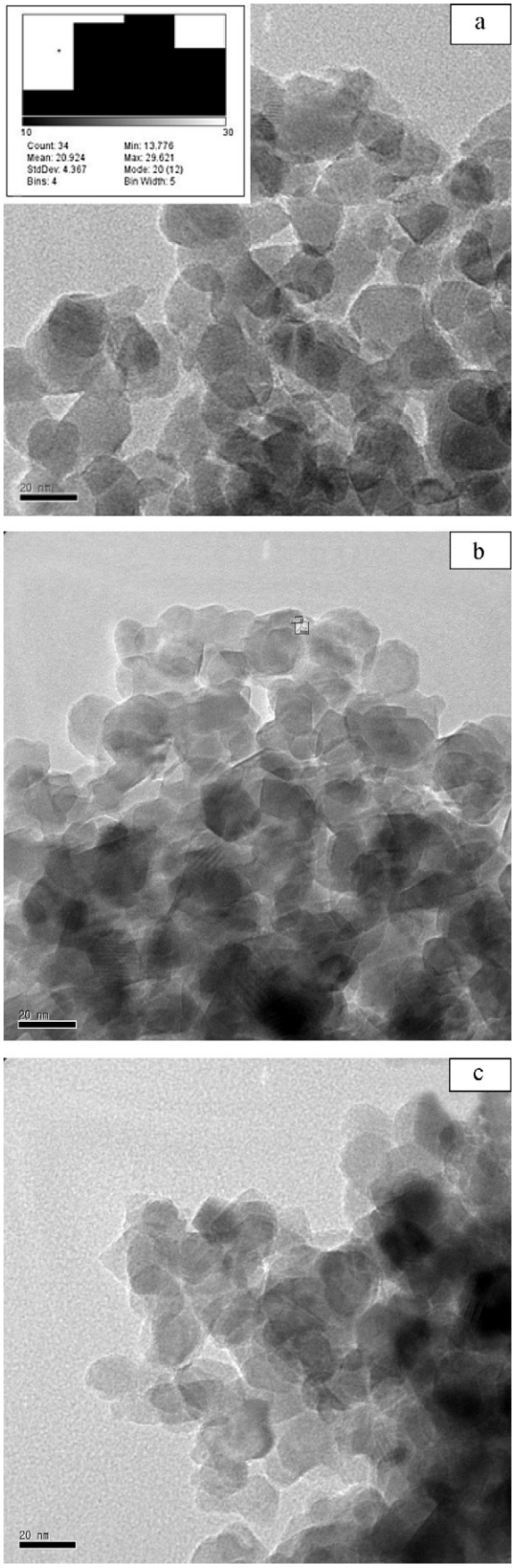

Fig. 2. TEM image of $MgFe_2O_4$ ferrite nanocrystals calcined at 600 °C. (a) Heptane (inset displays particle size distribution); (b) toluene; (c) cyclohexane.

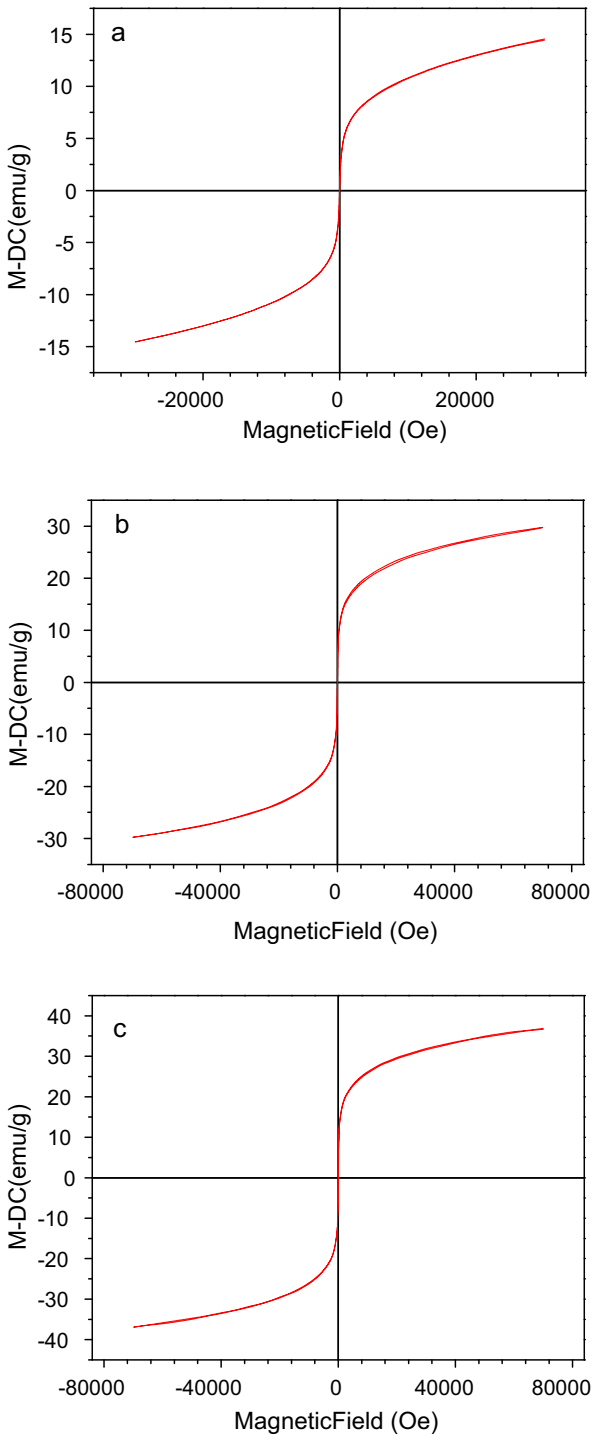

Fig. 3. Magnetization curves of $MgFe_2O_4$ ferrite nanocrystals calcined at 600 °C. (a) Heptane; (b) toluene; (c) cyclohexane

[26] produced $MgFe_2O_4$ nanocrystals at 900 °C from water in cyclohexane reverse micelle using Lutensol ON as surfactants with a saturation magnetization of 32 emu/g. However in the present study we were able to synthesize $MgFe_2O_4$ nanopowders at 600 °C from water in cyclohexane reverse micelle using Igepal CO 520 surfactant having higher saturation magnetization value of 37 emu/g. Though the saturation magnetization of $MgFe_2O_4$ prepared by milling process and solvothermal process are 39.3 emu/g [35] and 41.7 emu/g [36], the formation temperature (1400 °C (48 h), milling process) and particle size (300–800 nm, solvothermal process) is higher than our study.

4. Conclusions

The study demonstrates that continuous phase is found to affect the particle size, morphology and magnetic property. The average diameter of the particle prepared with heptane is 20.9 ± 4.3 nm. On the contrary, the product with toluene and cyclohexane is highly aggregated. Furthermore, these studies provide an excellent superparamagnetic nanoparticulate system in developing heating agents for magnetic hyperthermia application.

Acknowledgements

This research was supported by Basic Science Research Program through the National Research Foundation of Korea (NRF) funded by the Ministry of Education, Science and Technology (2010-0023003).

References

[1] G. Schmid, Nanoparticles: From Theory to Application, Wiley–VCH, Weinheim, 2004.
[2] K.J. Klabunde, Nanoscale Materials in Chemistry, Wiley-Interscience, New York, 2001.
[3] A.P. Alivisatos, Science 271 (1996) 933–937.
[4] C. Pacholski, A. Kornowsli, H. Weller, Angew. Chem. Int. Ed. 41 (2002) 1188–1191.
[5] T. Hyeon, Chem. Commun. 8 (2003) 927–934.
[6] M.P. Pileni, Nat. Mater. 2 (2003) 145–150.
[7] S. Mornet, S. Vasseur, F. Grasset, E. Duguet, J. Mater. Chem. 14 (2004) 2161–2175.
[8] Q. Chen, Z. John Zhang, Appl. Phys. Lett. 73 (1998) 3156–3158.
[9] T. Maehara, K. Konishi, T. Kamimori, H. Aono, H. Hirazawa, T. Naohara, S. Nomura, H. Kikkawa, Y. Watanabe, K. Kawachi, J. Mater. Sci. 40 (2005) 135–138.
[10] M. Ma, Y. Wu, J. Zhou, Y. Sun, Y. Zhang, N. Gu, J. Magn. Magn. Mater. 268 (2004) 33–39.
[11] J.H. Fendler, Chem. Rev. 87 (1987) 877–899.
[12] P.L. Luisi, B.E. Straub (Eds.), Reverse Micelles, Plenum, New York, 1984.
[13] S.E. Friberg, P. Bothorel (Eds.), Microemulsion: Structure and Dynamics:, CRC Press, Boca Raton, FL, 1987.
[14] A. Kale, S. Gubbala, R.D.K. Misra, J. Magn. Magn. Mater. 277 (2004) 350–358.
[15] M. Bellusci, S. Canepari, G. Ennas, A. La Barbera, F. Padella, A. Santini, A. Scano, L. Seralessandri, F. Varsano, J. Am. Ceram. Soc. 90 (2007) 3977–3983.
[16] C. Liu, B. Zou, A.J. Rondinone, Z. John Zhang, J. Phys. Chem. B 104 (2000) 1141–1145.
[17] R.D.K. Misra, A. Kale, B.J. Kooi, J.Th.M. De Hosson, Mater. Sci. Technol. 19 (2003) 1617–1621.
[18] S. Kumar, V. Singh, S. Aggarwal, U. Kumar Mandal, R. Kumar Kotnala, J. Phys. Chem. C (2010), doi:10.1021/jp911586d.
[19] M.D. Shultz, M.J. Allsbrook, E.E. Carpenter, J. Appl. Phys. 101 (2007) 09M518.
[20] V. Uskokovic, M. Drofenika, I. Ban, J. Magn. Magn. Mater. 284 (2004) 294–302.
[21] S. Thakur, S.C. Katyal, A. Gupta, V.R. Reddy, S.K. Sharma, M. Knobel, M. Singh, J. Phys. Chem. C 113 (2009) 20785–20794.
[22] S.A. Morrison, C.L. Cahill, E.E. Carpentera, S. Calvin, R. Swaminathan, M.E. McHenry Vincent, G. Harris, J. Appl. Phys. 95 (2004) 6392–6395.
[23] N. Sivakumara, A. Narayanasamy, J.-M. Greneche, R. Murugaraj, Y.S. Leed, J. Alloys Compd. 504 (2010) 395–402.
[24] P.P. Hankare, S.D. Jadhav, U.B. Sankpal, R.P. Patil, R. Sasikala, I.S. Mulla, J. Alloys Compd. 488 (2009) 270–272.
[25] T. Sasaki, S. Ohara, T. Naka, J. Vejpravova, V. Sechovsky, M. Umetsu, S. Takami, B. Jeyadevanc, T. Adschiria, J. Supercrit. Fluids 53 (2010) 92–94.
[26] P. Holec, J. Plocek, D. Niznansky, J.P. Vejpravova, J. Sol–Gel Sci. Technol. 51 (2009) 301–305.
[27] R.P. Bagwe, K.C. Khilar, Langmuir 13 (1997) 6432–6438.
[28] U. Natrajan, K. Handique, A.M. Mehra, J.R. Bellare, K.C. Khilar, Langmuir 12 (1996) 2670–2678.
[29] T.A. Hatton, A.S. Bommarius, J.F. Holzwarth, Langmuir 9 (1993) 1241–1253.
[30] J. Chandradass, K. Ki Hyeon, Adv. Powder Technol. 21 (2010) 100–105.
[31] S. Sun, H. Zheng, D.B. Robinson, S. Raoux, P.M. Rice., S.X. Wang, G. Li, J. Am. Chem. Soc. 126 (2004) 273–279.
[32] D. Yu, X. Sun, J. Zou, Z. Wang, F. Wang, K.J. Tang, J. Phys. Chem. B 110 (2006) 21667–21671.
[33] R.H. Kodama, J. Magn. Magn. Mater. 200 (1999) 359–372.
[34] C. Liu, B. Zou, A.J. Rondinone, Z.J. Zhang, J. Am. Chem. Soc. 122 (2000) 6263–6267.
[35] M.E. Rabanal, A. Varez, B. Levenfeld, J.M. Torralba, J. Mater. Proc. Technol. 143–144 (2003) 470–474.
[36] H. Deng, H. Chen, H. Li, Mater. Chem. Phys. 101 (2007) 509–513.